A Behaviour of a Catalyst Powder Flowing Down in a Dipleg

S. J. Wang[3], D. Geldart[2], M.S. Beck[3]* and T. Dyakowski[1]*

[1]Department of Chemical Engineering,
University of Manchester Institute of Science and Technology,
PO Box 88, Manchester M60 1QD, England

[2]Department of Chemical Engineering,
University of Bradford

[3]Department of Electrical Engineering and Electronics, UMIST

* The authors are members of the Virtual Centre for Industrial Process Tomography

Abstract *- The dipleg can generally operate in three basic flow regimes; packed-bed, fluidized- bed flow and a dilute flow called streaming flow. The most common perception of an overflow dipleg is that it consists of a fluidized dense phase at the bottom and a dilute phase in the upper part. This paper presents the tomographic images obtained at three locations along the dipleg. These show the effects of solids mass fluxes and the backpressure on the character of solids distribution along the pipe cross-section. The radial profiles of average solids distribution are compared with the literature data.*

Keywords: Capacitance Tomography, Circulating Fluidized Bed

1. INTRODUCTION

A primary cyclone dipleg is required in the circulating fluidized bed to allow the solids to flow from a relatively low-pressure region near the outlet from a cyclone to a high-pressure region at the bottom. The gravity force of solids is the driving potential for this transport. The solids are not supported by the gas flow (as in a riser) but fall, due to gravity resisted by the gas drag. Neglecting both the inlet and exit effects, the solids volume fraction in the dipleg is accompanied by higher solids velocity in the same region (solids cluster produces less drag per particle than isolated particles, (Yang, 1993).

Solids can flow through a dipleg in either dilute or dense phase flow. The direction of the actual gas flow relative to the dipleg wall can be either up or down and still has the relative gas-velocity direction upwards. As a result a flow pattern within a dipleg adjusts itself. Wachi and Yates (1991) as well as Wang et al. (1992) investigated the radial particle distribution in co-current flow and compared the profiles with those found in risers. According to Wang et al (1992) the radial profile in down flow conditions is more uniform than in risers. The particle tends to move to the wall, forming an annular region of high solids volume fractions between the centre and the wall. Close to the wall as well as in the centre, the solids volume fraction was found to be low. The radial solids velocity profile was similar to the low velocities in the centre and at the wall. The axial profiles of solids volume fraction, solids velocity and pressure present in down flow reactors were investigated by Zhu et al (1993). Generally, the knowledge obtained for the downer provides some valuable information to a flow pattern within a dipleg. This covers both a radial solids distribution as well as the solids mixing in axial and radial directions. However, it should be emphasised that the inlet within the downer is very carefully designed.

The aim of the present paper is to investigate the dynamic behaviour of gas-solids flow patterns at different levels at the dipleg. The effect of the inlet geometry on the flow pattern was studied for different solids mass fluxes. The images showing instantaneous solids distribution in a dipleg cross-section were obtained by use of the Electrical Capacitance Tomography (ECT) system. This system provided 200 images per second, and the data was processed to calculate time and cross-section average solids volume fraction distribution. Also, Peclet numbers characterizing mixing processes within a dipleg were calculated and compared with the available correlation.

2. EXPERIMENTS

A schematic diagram of the rig is shown in Figure 1. The dipleg is a Perspex pipe with 100-mm i.d. and 2.38 m long. At the top it is connected to the cyclone equipped with a diverter valve. At the bottom it is connected to a trickle valve. A rotary feeder, powered by an electronic

motor, fitted with a speed controller, delivers powder from the hopper into a 5" conveying line at solids feed rates up to about 5 kg s^{-1}. In order to allow calibration of the feeder, a measuring fluid bed is installed. During normal operation, powder flows out of the cyclone into the dipleg via a pneumatically operated diverter. In order to measure the circulation rate the solids are directed, for a specified number of seconds, into a 6" i.d glass column 1.5 m long fitted with a pipe grid distributor which fluidises the powder. The change in pressure drop across the bed is then used to calculate the mass of powder, which has been diverted. The hopper holds up to 150 kg powder, providing a residence time of 30 s at the maximum circulation rates, quite adequate to allow the powder to de-aerate. It is fitted with two thick flat Perspex windows, each with a thin sheet of glass on its inner surface to reduce electrostatic attraction and improve visibility.

The experiments were carried out using an equilibrium catalyst (E-Cat). This catalyst was a petroleum cracking catalyst, which was taken out of a cracking unit at Esso Fawley. The properties of the E-Cat powder, which could be classified as a Geldart group A powder, are listed in Table 1.

Weight average diameter [μm]	Solids density [kg m^{-3}]	Bulk density [kg m^{-3}]	Packed voidage [-]	Minimum fluidization Velocity [cm s^{-1}]
61.5	1750	881	0.497	0.14

Table 1. E-Cat powder properties.

The operation of the rig was continuous. During a run the solids were circulated through the rig at constant solid mass flux. Starting with the ball valve of the pipe fully open (0), the ball valve was then closed step by step to a closing angle of 60°. By closing the ball valve the release of gas from the tank was restricted, leading to a higher tank pressure. This stimulated the various backpressures possible in industrial plants depending, for instance, on the height of submersion of the dipleg in a fluidized bed. During the entire run the pressure drops in the system were recorded through the transducers. The solids in the rig were circulated many times during an experiment, hence avoiding bias between different runs due to inconsistent particle characteristics in the system. For all the experiments, the initial loading of solids in the storage tank was the same. The powder losses over a run to the bag filter were small in comparison to the total mass of solids in the system. During all the experiments the pulsating cleaning air of the bag filter was in operation to keep the pressure drop over the filter constant. These pulses were visible in the recordings, but from the experience of earlier work with the rig and from our observations, its influence on our further results was negligible. For each setting of the rotary feeder valve and each position of the pressure tapings / ECT at least two runs were carried out.

All the images were obtained by use of an 8-electrode single plane capacitance sensor with driven guard electrodes, Figure 1. The data presented show measurements obtained in the finite volume defined by the electrode height and the pipe diameter. Therefore, all the images are averaged along the electrode height, and in this way the term ‘cross-section’ slice should be understood.

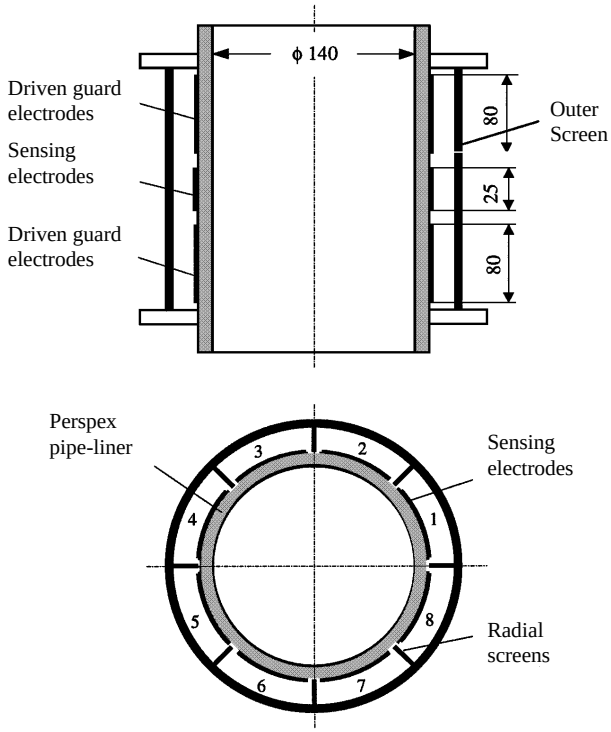

Figure 1. Diagram of the 8-electrode single-plane capacitance sensor with guard electrodes.

3. FLOW PATTERNS IN THE DIPLEG

As shown in Figure 2 the top of the dipleg was connected via a short chute with a cyclone. The solids leaving the cyclone were falling on the bottom surface of the chute and were moving down. Therefore, the solids at the inlet to the dipleg were non-uniformly distributed and occupied only a part of the dipleg circumference. At the bottom of the dipleg a trickle valve was mounted to prevent upward bypass gas flow within the dipleg. This valve has a comparatively large opening section and hence allows high-mass fluxes of solids to discharge.

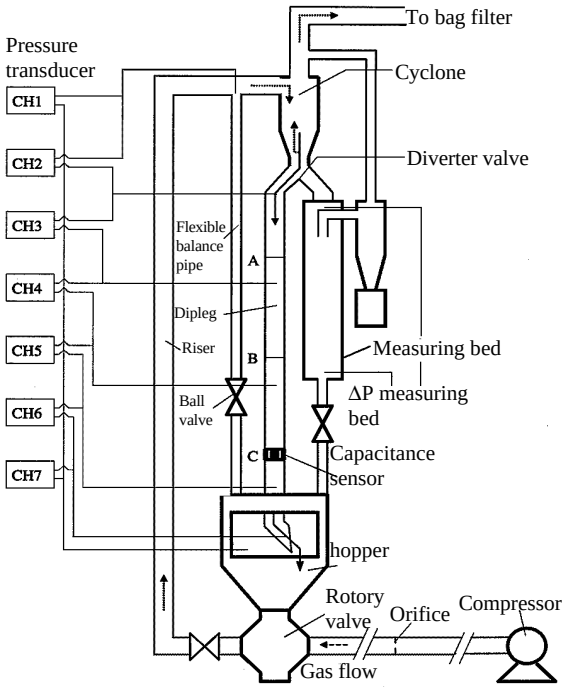

Figure 2. Schematic diagram of the experimental primary cyclone dipleg with the capacitance sensor.

3.1 Instantaneous solids volume fraction distribution

An example of a set of instantaneous images is shown in Figure 3. Letters E and F (Figure 3(a)) depict a projection of the common edge between the chute and the dipleg. A majority of the instantaneous images obtained at level A shows that the high solids volume fraction region existed were around the line EF. A low solids volume fraction region existed almost opposite this line. A small amount of solids was injected in the form of a solids jet which hit the opposite wall. This seems to be caused by some fluctuations in the riser-dipleg system which, in turn, generated an increase in solids velocity at the inlet to the dipleg.

The solids falling down distribute themselves into an annular shape round the wall and during the same time into the centre of the dipleg. As shown at level B (Figure 3(b)) the solids are more uniformly distributed along the dipleg circumference and the region of the highest solids concentration appears at the various locations along the dipleg circumference. Additionally, the solids presence at the centre of the dipleg results from a radial solids motion between levels A and B.

As expected, the solids at level C were even more uniformly distributed and the size of the high solids concentration is larger than at level B. This indicates the de-fluidization caused by the increase in the pressure at the bottom of the dipleg, (Figure 3(c)).

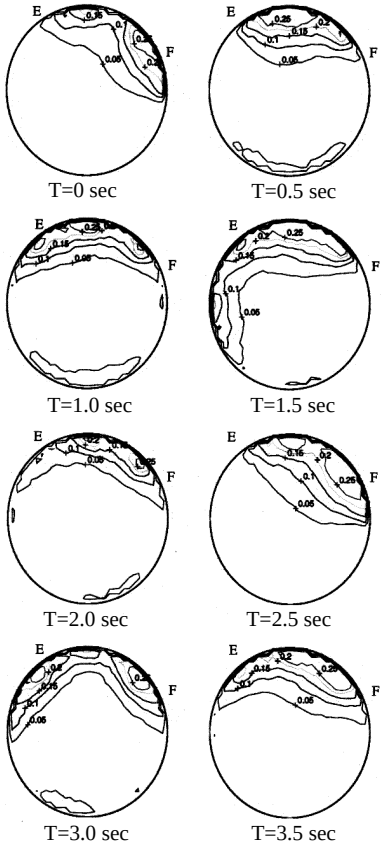

Figure 3a. A Sequence of instantaneous images at level A in the dipleg, G_s=269 kg m^{-2} s^{-1}, backpressure, ΔP_b=3568 Pa.

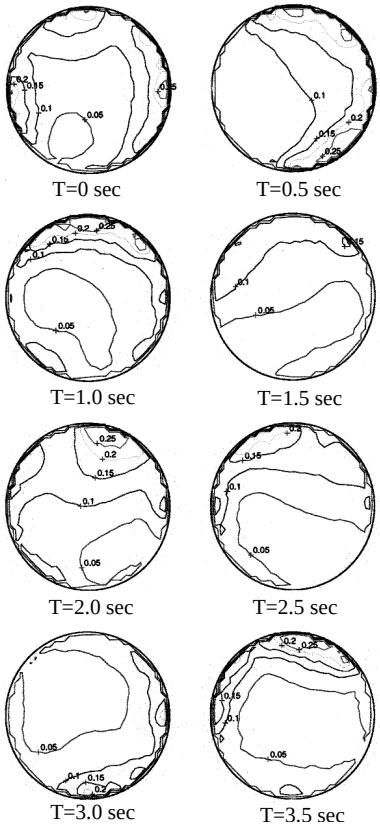

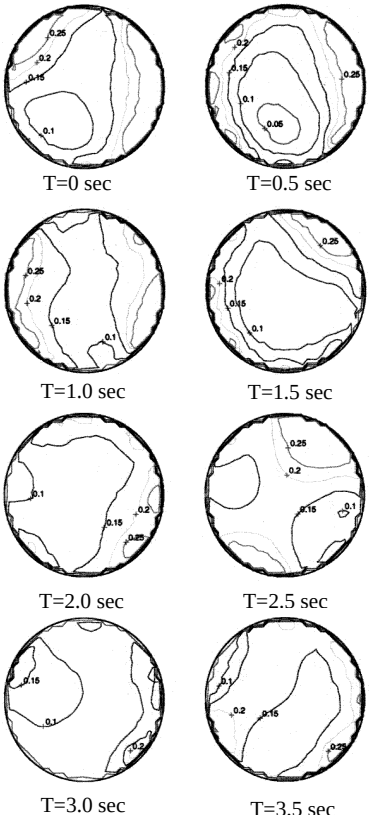

Figure 3b. A Sequence of instantaneous images at level B in the dipleg,G_s=269 kg m^{-2} s^{-1}, backpressure, ΔP_b=3568 Pa.

Figure 3c. A Sequence of instantaneous images at level C in the dipleg,G_s=269 kg m^{-2} s^{-1}, backpressure, ΔP_b=3568 Pa.

3.2 Time average solids volume fraction distribution

Time average tomograms, which were calculated from 1000 instantaneous images, are presented in Figure 4. These reflect the discussed instantaneous changes in the solids

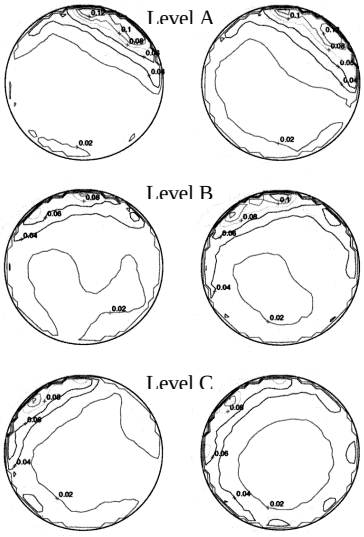

(c) Back pressure, ΔPb=596Pa (d) Back pressure, ΔPb=1052Pa

distribution along the dipleg. Generally, the time

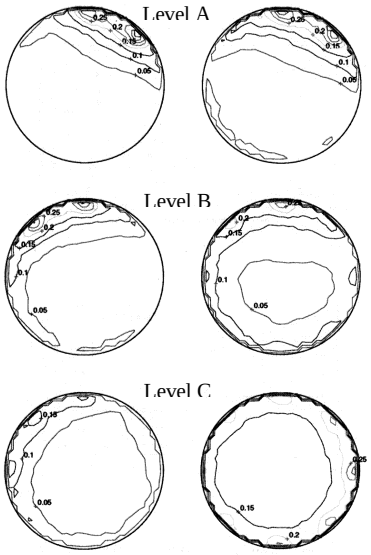

(a) Back pressure, ΔPb=596Pa (b) Back pressure, ΔPb=1052Pa

average solids volume distribution exhibits a non-axisymmetrical pattern even at the lowest location, which might be caused by the effect of the exit.

Figure 4a. Time averaged solids volume fraction distribution, solids flux, G_s=111 kg m^{-2} s^{-1}.

Figure 4b. Time averaged solids volume fraction distribution, solids flux, G_s=269 kg m^{-2} s^{-1}.

3.3 Time and cross-section average solids volume fraction distribution

The average solids volume fractions in the dipleg cross-section were calculated applying the procedure fully explained in Wang [5]. The variations of solids volume fractions as a function of the dipleg length and the backpressure are illustrated in Figure 5. As shown in this figure the solids volume fraction increases significantly along the dipleg length only for the higher solids mass fluxes and the higher backpressure values. The solids volume fraction almost doubles for solid mass flux 320 kg m^{-2} s^{-1} and the maximum backpressure. For both smaller solids mass fluxes and the backpressure only a very modest increment in the solids volume fraction was noticed. Therefore, the results presented do not fully support a common perception that an overflow dipleg consists of a fluidized dense phase at the bottom and a dilute phase in the upper part.

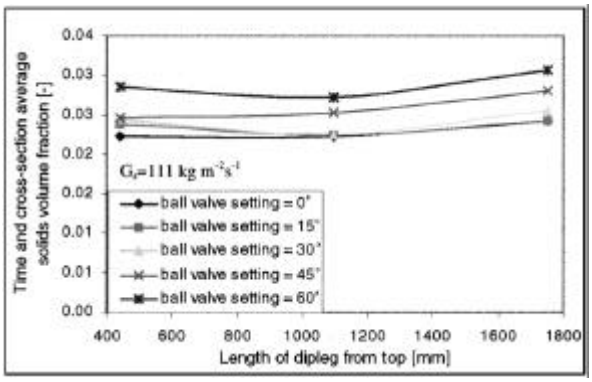

Figure 5a. Average solids volume fraction vs. length of dipleg, G_s=111 kg m^{-2} s^{-1}

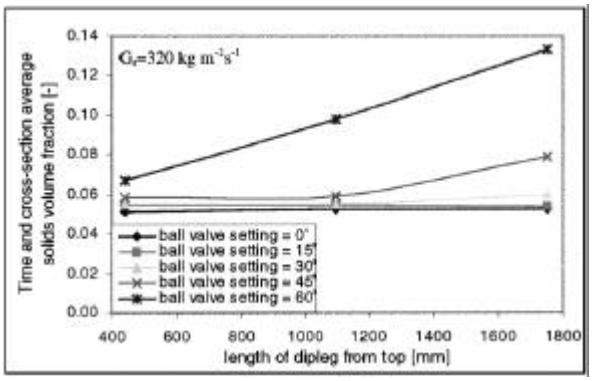

Figure 5b. Average solids volume fraction vs. length of dipleg, G_s=320 kg m^{-2} s^{-1}.

Time average solids distribution along the radius can be split into three regions (Zhu et al., 1995): the wall region, the annulus region and the core region. In the core region, solids volume fractions and their velocities are nearly uniform; in the annulus solids concentrations and velocities are larger than in the core and close to the wall both velocities and concentrations are decreasing. The solids volume fraction distributions were calculated using the following correlation:

$$ {}^{T} = {}^{A,T}\,F( ) \qquad (1) $$

Superscripts T and A, T means time average and cross-sectional and time average values, respectively. Function F ( ) is defined by the following equation:

$$ F( ) = 30.62\,(1-) \quad \exp[-127.6(1-)^{2}] + 22.8/\{36.7 + (1-)\} \qquad (2) $$

and = r/R is a dimensionless radius

The results presented in Figure 6 show the same pattern of solids distributions as those obtained from equation 1, except the wall region. The ECT data may underestimate the gradient of solids distribution close to the boundary between the core and annulus. This seems to be caused by blurring effects in the reconstruction algorithm.

The solids mixing both in axial and radial directions can be characterized by the corresponding Peclet numbers. These were calculated from the following equation:

$$ Pe_a = 8.93\times10^{-7}\,Re\,/(1 - {}^{A,T}) + 101 \qquad (3) $$

and

$$ Pe_r = 140\,Re^{0.61}\,(1 - {}^{A,T})^{1.23} \qquad (4) $$

Where Re is the Reynolds number.

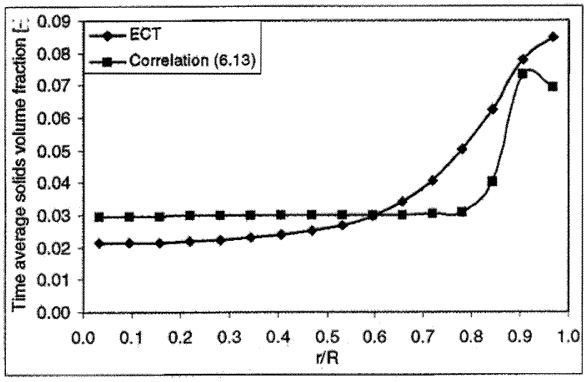

(a) Gs=225 Kg $m^{-2}s^{-1}$

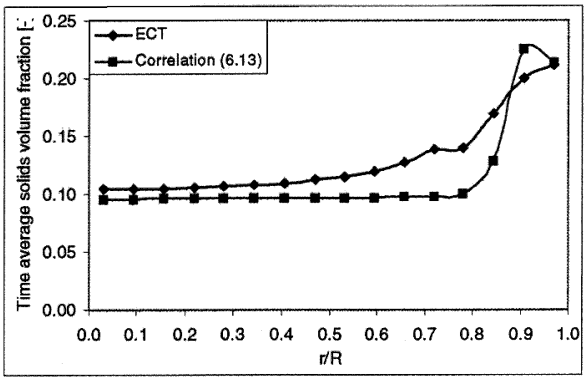

(b) Gs=269 Kg $m^{-2}s^{-1}$

Figure 6. Comparison of ECT measurements with the Correlation (6.13).

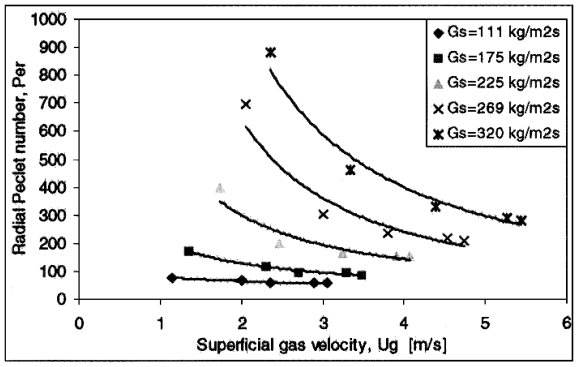

(a) Radial Peclet number

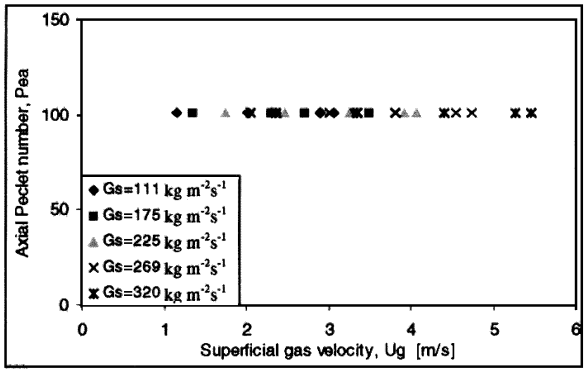

(b) Axial Peclet number

Figure 7. Peclet number in the dipleg.

The results are presented in Figure 7. The radial Peclet number is increasing with the solids volume fraction. Therefore, an increase of a gas solid superficial velocity (at constant solids mass flux) reduces the radial mixing. This is also congruent with the average images presented in Figure 4. The axial Peclet numbers are nearly the same, which show that the axial mixing is not affected by the gas velocity

4. CONCLUSIONS

The ECT system was applied for imaging gas-solids flow patterns within a dipleg. Solids falling down a primary cyclone distribute themselves from an early strand into an annular shape around the wall of the dipleg and during the same time into the centre of the dipleg. The solids migration along the dipleg circumference reduces the maximum solids volume fraction and results in more uniform solids distribution along the dipleg circumference. Solids volume fraction along the length of dipleg and Peclet numbers characterizing mixing processes were calculated from tomograms. Except for the wall region, the results obtained from the tomograms show the same pattern of solids distributions as those obtained from the literature correlations

REFERENCES

[1] W. C. Yang, *The hydrodynamics of circulating fluidized beds*, In: Encyclopaedia of Fluid mechanics, - Supplement 2: Advances in Multiphase flow (ed. N. P. Cheremisinoff), Gulf Publishing Company, Houston, Texas, 1993, pp. 29-346.

[2] S. Wachi and J.G. Yates, *Downward lean flow in a vertical tube*, Chem. Eng. Sci., **46**, pp. 929-937, 1991.

[3] Z. Wang, D. Bai, and Y. Jin, *Hydrodynamics of co-current circulating fluidized bed*, Powder Technol., **70**, p. 271-275, 1992.

[4] J.X. Zhu, Z. Q. Yu, J.R. Grace and A. Issangya, *Co-current down-flow circulating fluidized bed (downer) reactor* – A state of the art review, Can. J. Chem. Eng., **73**, pp. 662-677, 1995

[5] S.J. Wang, *Measurement of Fluidization Dynamics in Fluidized beds Using Capacitance Tomography*, PhD thesis, UMIST, 1998.